A Deep Dive into the Delta Wave: Forecasting SARS-CoV-2 Epidemic Dynamic in Poland with the pDyn Agent-Based Model

Karol Niedzielewski (kniedzie@icm.edu.pl)
Interdisciplinary Centre for Mathematical and Computational Modelling, University of Warsaw, https://orcid.org/0000-0001-7405-2207

Rafał P. Bartczuk
Interdisciplinary Centre for Mathematical and Computational Modelling, University of Warsaw, https://orcid.org/0000-0002-0433-7327

Natalia Bielczyk
Ontology of Value https://orcid.org/0000-0003-1604-9143

Dominik Bogucki
Interdisciplinary Centre for Mathematical and Computational Modelling, University of Warsaw, https://orcid.org/0009-0000-9473-2242

Filip Dreger
Interdisciplinary Centre for Mathematical and Computational Modelling, University of Warsaw, https://orcid.org/0000-0003-1812-8216

Grzegorz Dudziuk
Interdisciplinary Centre for Mathematical and Computational Modelling, University of Warsaw,

Łukasz Górski
Interdisciplinary Centre for Mathematical and Computational Modelling, University of Warsaw, https://orcid.org/0000-0003-0871-6575

Magdalena Gruziel-Słomka
Interdisciplinary Centre for Mathematical and Computational Modelling, University of Warsaw, https://orcid.org/0000-0001-6882-7408

Jędrzej Haman
Interdisciplinary Centre for Mathematical and Computational Modelling, University of Warsaw,

Artur Kaczorek
Interdisciplinary Centre for Mathematical and Computational Modelling, University of Warsaw, https://orcid.org/0000-0002-4752-4480

Jan Kisielewski
Faculty of Physics, University of Bialystok https://orcid.org/0000-0002-1082-4324

Bartosz Krupa

Interdisciplinary Centre for Mathematical and Computational Modelling, University of Warsaw, https://orcid.org/0000-0002-2958-2046

Antoni Moszyński
Interdisciplinary Centre for Mathematical and Computational Modelling, University of Warsaw, https://orcid.org/0000-0003-0128-7384

Jędrzej M. Nowosielski
Interdisciplinary Centre for Mathematical and Computational Modelling, University of Warsaw, https://orcid.org/0000-0002-9627-3008

Maciej Radwan
Interdisciplinary Centre for Mathematical and Computational Modelling, University of Warsaw, https://orcid.org/0000-0001-5789-316X

Marcin Semeniuk
Interdisciplinary Centre for Mathematical and Computational Modelling, University of Warsaw, https://orcid.org/0000-0002-3136-7249

Urszula Tymoszuk
Division of Psychiatry, University College London https://orcid.org/0000-0002-0781-2752

Jakub Zieliński
Interdisciplinary Centre for Mathematical and Computational Modelling, University of Warsaw, https://orcid.org/0000-0001-8935-8137

Franciszek Rakowski
Interdisciplinary Centre for Mathematical and Computational Modelling, University of Warsaw, https://orcid.org/0000-0001-6133-8900

Research Article

Keywords: epidemic dynamics, epidemiology, agent-based model, COVID-19

Posted Date: May 23rd, 2023

DOI: https://doi.org/10.21203/rs.3.rs-2966996/v1

A Deep Dive into the Delta Wave: Forecasting SARS-CoV-2 Epidemic Dynamic in Poland with the pDyn Agent-Based Model

Karol Niedzielewski[1*], Rafał P. Bartczuk[1,2*], Natalia Bielczyk[3], Dominik Bogucki[1], Filip Dreger[1], Grzegorz Dudziuk[1], Łukasz Górski[1], Magdalena Gruziel-Słomka[1], Jędrzej Haman[1], Artur Kaczorek[1], Jan Kisielewski[1,4], Bartosz Krupa[1], Antoni Moszyński[1], Jędrzej M. Nowosielski[1], Maciej Radwan[1], Marcin Semeniuk[1], Urszula Tymoszuk[5], Jakub Zieliński[1], Franciszek Rakowski[1]

[1*]Interdisciplinary Centre for Mathematical and Computational Modelling, University of Warsaw, Tyniecka 15/17, Warsaw, 02-630, mazowieckie, Poland.
[2*]Institute of Psychology, John Paul II Catholic University of Lublin, Al. Racławickie 14 (C-443), Lublin, 20-950, lubelskie, Poland.
[3*]Ontology of Value, Veldstraat 48, Nijmegen, 6533CD, Netherlands.
[4*]Faculty of Physics, University of Bialystok, Ciołkowskiego 1L, Białystok, 15-245, podlaskie, Poland.
[5]Division of Psychiatry, University College London, Maple House, 149 Tottenham Ct Rd, London, W1T 7BN, Great Britain.

*Corresponding author(s). E-mail(s): k.niedzielewski@icm.edu.pl; bartczuk@icm.edu.pl;
Contributing authors: ; db443201@icm.edu.pl; fdreger@gmail.com; dudziuk@icm.edu.pl; lgorski@icm.edu.pl; magd@icm.edu.pl; jedrzej.haman@gmail.com; a.kaczorek@icm.edu.pl; jankis@uwb.edu.pl; bk437917@icm.edu.pl; amos@icm.edu.pl; jnow@icm.edu.pl; mradwan@icm.edu.pl; xahil@icm.edu.pl; ; jziel@icm.edu.pl; rakowski@icm.edu.pl;

Abstract

In this work, we describe and forecast the fourth wave of the SARS-CoV-2 epidemic, driven by the Delta variant, using pDyn — a detailed epidemiological agent-based model. It is designed to explain the spatiotemporal dynamics of the SARS-CoV-2 spread across Polish society, predicting the number and locations of disease-related states for agents living in the virtual society in response to varying properties of the pathogen and the social structure and behavior.

We evaluate the validity of the dynamics generated by the model, including the succession of pathogen variants, immunization dynamics, and the ratio of vaccinated individuals among confirmed cases. Additionally, we assess the model's predictive power in estimating pandemic dynamics (peak timing, peak value, and wave length) of disease-related states (number of confirmed cases, hospitalizations, ICU hospitalizations, and deaths) both at the national level and in the highest administrative units in Poland (voivodships).

When testing the model's validity, we compared real-world data (excluding data used for calibration) to our model estimates to evaluate whether pDyn accurately reproduced the epidemic dynamics up to the simulation time (October 28, 2021). To assess the accuracy of pDyn's predictions, we retrospectively compared simulation results with real-world data acquired after the simulation date, evaluating pDyn as a tool for predicting future epidemic spread.

Our results indicate that pDyn accurately predicts and can help us better understand the mechanisms underlying the SARS-CoV-2 dynamics.

Keywords: epidemic dynamics, epidemiology, agent-based model, COVID-19

1 Introduction

The first confirmed case of coronavirus disease 2019 (COVID-19) in Poland was identified on March 4, 2020, approximately a month later compared to Western Europe countries [1] (cf. 1 (a)). On March 10, the World Health Organization declared the local transmission phase of severe acute respiratory syndrome coronavirus 2 (SARS-CoV-2) in Poland [2]. Two days later, the first COVID-19-related death in Poland, a 56-year-old woman, was reported [3]. As the epidemic spread throughout the country, the Polish government declared a state of epidemic emergency, and subsequently, the epidemic state, enabling the introduction of epidemic mitigation policies [2] (see Figure 1 (d)). The critical pharmaceutical and non-pharmaceutical interventions (NPIs) introduced in Poland between March 4, 2020, and December 31, 2021, to combat the spread of SARS-CoV-2 are listed in Table S1.1 in the Supplementary material. Primarily, following the detection of the first COVID-19 case, the Polish government introduced obligatory isolation of infected persons, quarantine of exposed contacts (including basic contact tracing), and SARS-CoV-2 testing. A range of public social distancing measures, including public gathering bans as well as school and workplace closures, were also implemented starting from the second week of March 2020, with the national lockdown announced on March 24, 2020. Additional indoor

and outdoor face-covering mandates were enacted on March 30 and April 14, 2020. The national COVID-19 vaccination program commenced on December 27, 2020.

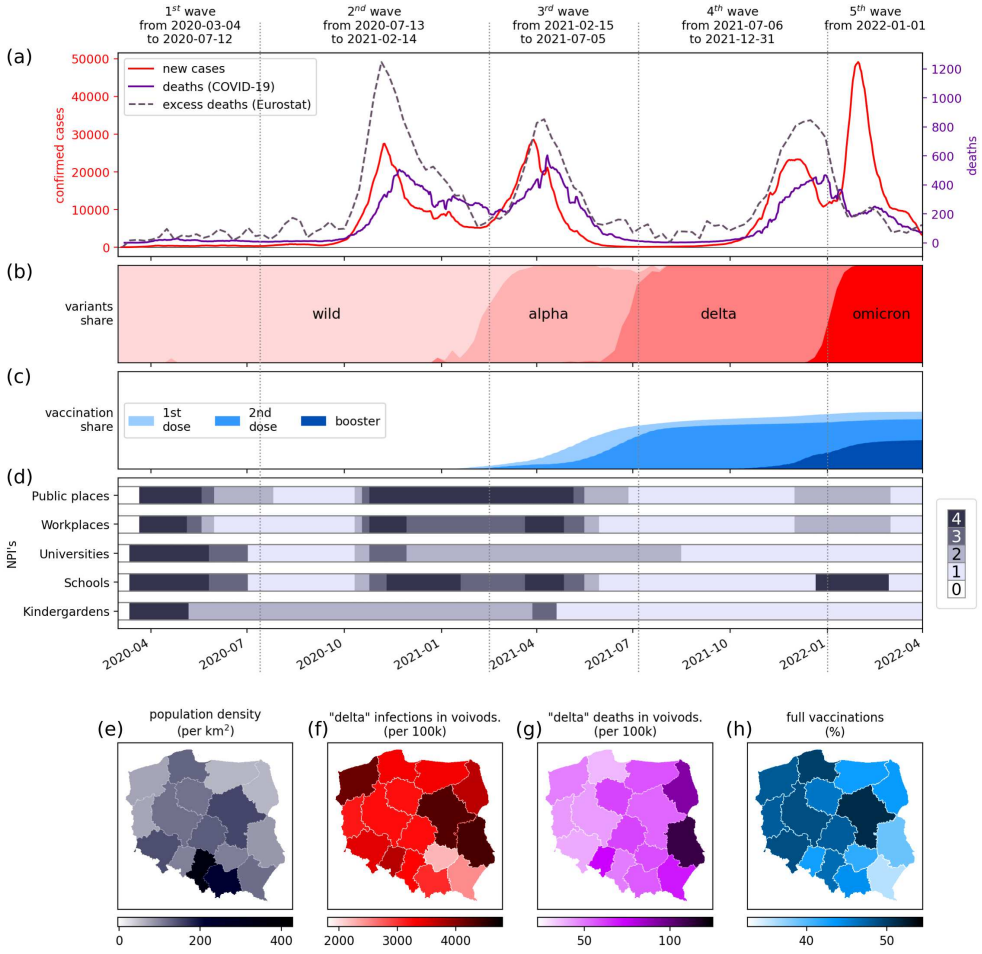

Fig. 1 Timeline of SARS-CoV-2 epidemic in Poland. (a) The epidemic curve showing the progression of reported daily new confirmed cases in Poland (red), number of COVID-19-related deaths (purple), and excess deaths (dashed). (b) Proportions of dominating variants. (c) Full vaccination share. (d) Government mitigation measures by implementation areas and ranks of restrictive strength. (e) Map of inhabitants density in voivodships. (f) Map of reported cases during the Delta wave in voivodships. (g) Map of deaths during the Delta wave in voivodships. (h) Map of vaccinations per 100,000 inhabitants in voivodships up to May 2022. Data sources: daily cases, COVID-19-related deaths and vaccinations: Ministry of Health; excess deaths: Eurostat; variants: GISAID; restrictions: own elaboration based on governmental information (see S1.1.

The ongoing evolution of the epidemic dynamic (e.g., the emergence of new virus variants, seasonal shifts in transmission rates, regional outbreaks, and introduction of

vaccinations) required a dynamic approach to epidemic mitigation strategies (including localized and reactive implementation modes). For instance, a reactive policy regarding school closures and remote working mandates based on defined thresholds of the number of cases per 10,000 inhabitants in administrative units was applied on August 7, 2020. Also, the adherence to the prevention and control measures varied with time, by socio-demographic factors and location. For instance, the compliance with face mask use was different for older vs. younger adults, urban vs. rural locations, and throughout the epidemic [4, 5]. In addition, ever-emerging evidence about SARS-CoV-2 pathogen properties (i.e., mode of transmission, the infectivity of asymptomatic cases, naturally induced immunity and its' waning over time, risk of reinfections) further contributed to the complexity of SARS-CoV-2 spread forecasting.

As a result, the need to manage SARS-CoV-2 transmissions has increased the demand for accurate forecasts, including new infections, hospitalizations in general and intensive care units (ICUs), and COVID-19-related deaths.

Agent-based models (ABMs) are a robust method for modeling infectious disease spread for over 30 years [6, 7]. They directly represent a dynamic social network of agents and the heterogeneity of their interactions in georeferenced locations [8–10]. ABMs rely on a synthetic society reflecting the demographic structure and population densities of a given territory [11]. They require input from a georeferenced network of sites where agents can operate and interact, including households, schools, workplaces, and public spaces (so-called contexts). ABMs as generative models enable to recreate complex phenomena during outbreaks, accounting for regional variations, demographic structure, behavioral reactions, and calibrating parameters to a lower spatial scale. In contrast, data-based, phenomenological models (such as uniform mixing compartment models) lack implicit interactions between significant factors such as virus variants or social structure networks [12].

The Ferguson group model [13] remains a textbook ABM approach for modeling infectious disease processes. It was initially used to simulate influenza spread and predict the effectiveness of targeted antiviral prophylaxis in Southeast Asia. The model represents society by grouping individuals into households with distinct generational layers. In 2020, it was adapted to predict SARS-CoV-2 spread by adjusting disease parameters to reflect the virus's characteristics [14]. These predictions guided the intermittent lockdown strategy in the UK, known as "The Hammer and the Dance" [15].

Our first model coined pDyn (from *pandemics dynamics*, developed in 2008 to describe influenza spread scenarios in Poland [16, 17], was inspired by Ferguson group model [13]. For the COVID-19 epidemic, we adapted the simulation platform to accommodate the specific characteristics and requirements of decision-makers based on the demands of the situation. The pDyn model [18] is capable of simulating and forecasting various SARS-CoV-2 transmission scenarios. It has been officially endorsed by the government, along with the MOCOS model [19] and the Ministry of Health Department of Analysis and Strategy model, as one of the primary tools for providing scientific explanations and forecasts of the epidemic processes to policymakers and medical advisory councils on a long-term basis.

In Poland, several ABM models were developed. Compared to the MOCOS model, pDyn has a detailed and georeferenced structure of various contexts [19], while MOCOS implements advanced contact-tracing analytical methods. Other models, such as those developed as concept models [20, 21], provided valuable methodological scientific insights but were only used locally and did not reach an operational regime.

During the first year of the pandemic, the pDyn model was one of the few robust models validated against real-world data. A systematic review of 126 SARS-CoV-2 ABMs revealed that only 17% were validated against real-world data, 3% were compared with other models, and 2% were systematically tested [22]. Furthermore, pDyn has continuously undergone external validation with real-world data [23] as part of the German and Polish COVID-19 Forecast Hub since November 2020 [24, 25]. Individual ABMs, MOCOS [19] and pDyn, have achieved significant performance improvements in long-term case forecasting in Poland due to their meticulous tailoring to specific country situations [25].

Agent-Based Models, such as pDyn, have proven effective in modeling and predicting epidemics by serving as virtual laboratories that enable the formalization and testing of epidemic dynamics. Unlike models that rely on general factors and variable aggregates, ABMs concentrate on modeling agents and their interactions, enabling the formulation of theories at the agent level, identifying necessary principles and assumptions, and revealing gaps in research and inconsistencies in theoretical systems [8, 9, 26]. Consequently, the ABM's prediction ability depends on accurately reflecting elementary epidemic processes and supporting hypotheses on their impacts on real-world data [8–10]. However, ABMs' implementation of complex epidemic processes and fidelity to real-world rules come at a cost, requiring numerous parameters and high computational expenses. Additionally, the calibration process demands significant resources, making reliable calibration a non-trivial issue [9, 10, 27].

This report forecasts the spatiotemporal dynamics of the COVID-19 epidemic in Poland using ABM pDyn. Our methodology incorporates multiple factors, including disease transmission, disease course, and epidemic course (see Figure 8 in Methods 4). Disease transmission considers the characteristics of multi-variant pathogens, partial immunity, and the role of social contacts. The course of the disease includes detailed disease-related states, age dependency, and dark figure estimation. Finally, the course of the epidemic considers changes in risk exposure due to NPIs, periodic behavioral changes, vaccination policies, cross-immunity, and immunity waning. Eventually, we evaluate the validity of the dynamics implemented in our model by emphasizing consistency with real-world data not used for calibration.

In this analysis, we cover the period from the onset of the epidemic until the end of 2021. During this time, Poland experienced four SARS-CoV-2 epidemic waves. The first and second waves (March 4, 2020 - July 12, 2020, and July 13, 2020 - February 14, 2021, respectively) were predominantly driven by the wild-type virus variant, followed by the third Alpha variant wave (February 15, 2021 - July 5, 2021), and the fourth Delta variant wave (July 6, 2021 - December 31, 2021), resulting in a total of 4,106,914 SARS-CoV-2 cases, 96,967 COVID-19 related deaths, and 173,376 total excess deaths reported in Poland [28] (see Figure 1 (a) and (b)).

The forecast, formulated on October 28, 2021, used pDyn [18] to focus on the fourth (Delta) wave of the epidemic in Poland, which marked the end of the process of obtaining herd immunity. This wave was unique in falling spontaneously, without restrictions or limiting contacts. Subsequent waves in 2022 were reinfection waves carrying lower risks of severe conditions and deaths due to weaker susceptibility to new variants. However, as the forecast was made before the Omicron wave emerged in January 2022, it was not included in the analysis due to the lack of information on the variant at the time.

The specific objectives of this study were: (1) to evaluate the validity of the dynamics implemented in the pDyn model, (2) to assess its ability to predict disease-related states' dynamics on a national level, and (3) to assess its ability to predict epidemic dynamics in the highest administrative units in Poland (voivodships) using data reported on the national level. We compared real-world data on SARS-CoV-2 variants, immunization dynamics, and the ratio of vaccinated individuals among confirmed cases to our model estimates to evaluate the model's validity. We also compared the results obtained in the simulation with real-world data acquired after the simulation date to test pDyn's predictive accuracy. In addition, we assessed regional forecasts made using data reported on the national level, taking into account the synthetic society's reflection of the geographical variation in the social-demographic structure of the Polish population.

As presented further, the generative, epidemiology-driven dynamic approach of pDyn allowed for achieving high predictive power when modeling the spread of COVID-19 epidemics.

2 Results

2.1 Dominating variant of pathogen

Before the day of our simulation, three dominant variants had been detected in Poland (namely, the wild type, Alpha, and Delta). In Fig. 2 on the panel [a], one can observe the distribution of three variants (wild type [blue], Alpha [orange], and Delta [green]) among infected agents. Panel [b] compares the model's variant succession dynamics with the real-world dataset from GISAID. This investigation did not include the Omicron variant's prevalence as it was not part of the October 2022 forecast.

The GISAID data is based on samples of varying sizes, and it is likely to be biased given that the samples for Poland are small (see Fig. 2 [c]). Therefore, only comparing the relative prevalence of a variant expressed as a percentage is possible. To validate our results, we compared the timing of the variant succession in 25%, 50%, and 75% percentile thresholds.

Our pDyn model reached 25% of the Alpha variant one week after the reference GISAID results, while 50% and 75% of the Alpha variant were reached two weeks after the reference GISAID results.

As for the Delta variant, the model reached 25% two weeks after the reference GISAID results, 50% three weeks after, and 75% four weeks after the reference GISAID results.

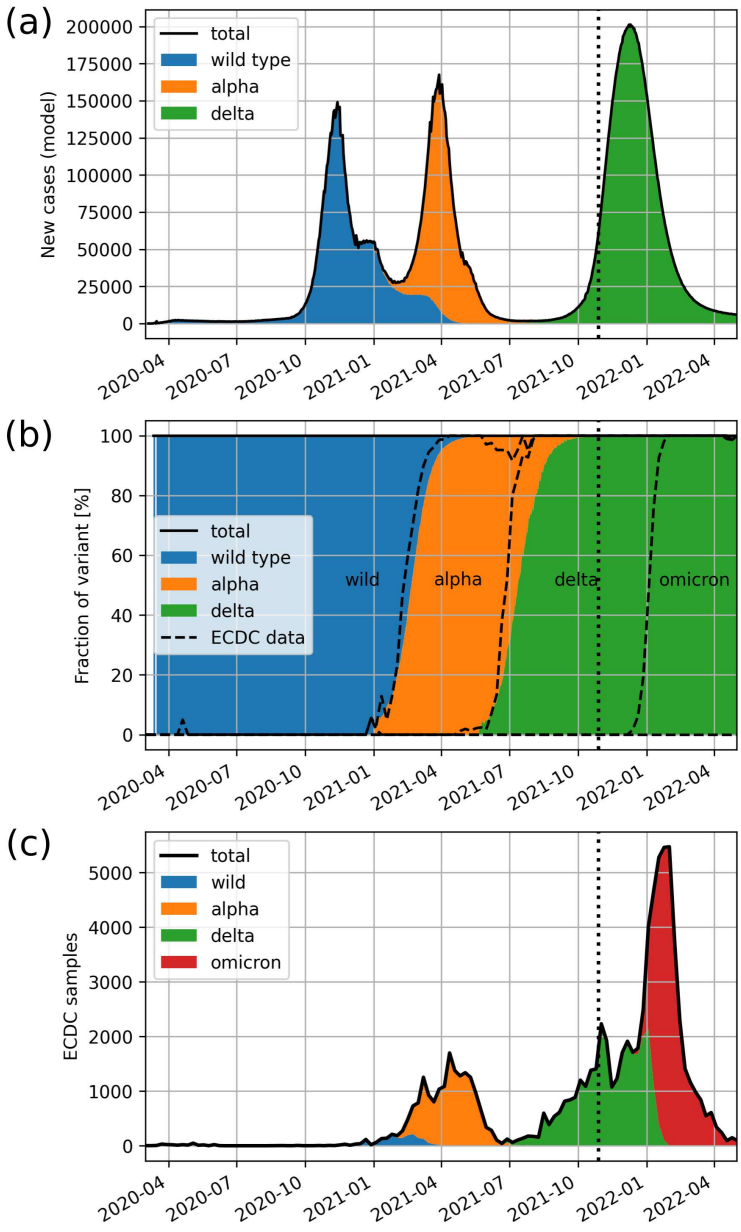

Fig. 2 Comparison of the dynamics of a succession of SARS-CoV-2 variants obtained from the pDyn model (colors) with the dataset obtained from GISAID study [29] (dashed lines). All the data is aggregated in weekly intervals. The vertical dotted line marks the simulation date.

It is worth mentioning that the transition from the Alpha to Delta variant in Poland occurred while there was a relatively low number of new detected cases. Hence, we consider our succession of the Delta variant as realistic.

2.1.1 Immunization level

In Fig. 3, we can observe the entire course of immunization level dynamics as shown by the pDyn model during the epidemic with the separation of immunization sources: disease, vaccination, and total. The model results were compared to the four-round OBSER-CO nationwide seroprevalence study maintained by the National Institute for Public Health in Poland [30].

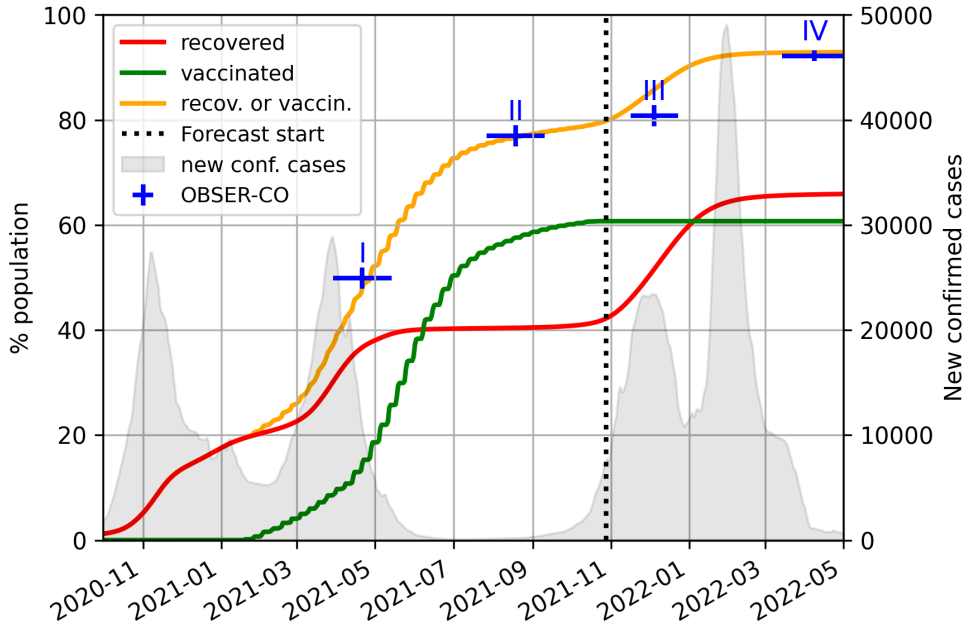

Fig. 3 Comparison of immunization dynamics between the model output and four rounds of the OBSER-CO study 3. The lines show the cumulative percentage of the agents' population (left axis) that is either recovered [red], vaccinated [green], or recovered or vaccinated [yellow], based on the model's results. The blue markers indicate the estimated fraction of the population with SARS-CoV-2-specific antibodies from four rounds (I-IV) of the OBSER-CO study. The horizontal marker line denotes the duration of each round, while the vertical marker line represents the 95% confidence interval of the estimate. A vertical dotted line indicates the simulation date. The transparent grey shape in the background represents the number of real-world confirmed cases (right axis).

As presented in Fig. 3, the cumulative sum of recovered and vaccinated agents predicted by the model comes close to the estimates from the seroprevalence study at all four checkpoints. These estimates (model vs. data, given as a percentage of the entire population) were as follows: 48.1 vs. 49.9 (95%CI [47.9; 51.9]) in April/May

2021, 76.8 vs. 77.0 (95%CI [75.0; 79.0]) in September 2021, 85.8 vs. 80.8 (95%CI [78.8; 82.8]) in December 2021, and 92.9 vs. 92.2 (95%CI [91.2; 93.2]).

Rounds I and II of the OBSER-CO study fall on the calibration stage of the simulation, while the model results for rounds III and IV are purely prognostic values. Keeping in mind that OBSER-CO data on seroprevalence (based on levels of antibodies in the trial groups) are not precisely the same indicator as a sum of recovered and vaccinated cases obtained from the model, it is still remarkable how well the model approximates immunity in the society. This knowledge is essential for reaching a reliable forecast of consecutive epidemic waves.

2.1.2 Fraction of vaccinated detected cases

The third validation concerns the number of vaccinated subjects among all infected subjects, which we refer to as the "fraction of vaccinated detected cases." As described in Methods 4, the model adopted a vaccination strategy based on governmental data: the number of vaccinated agents at the given age, time, and location. At the same time, the dynamics of the fraction of vaccinated detected cases is an emergent property that can be compared to real-world data (the data was obtained from the government under NDA). The comparison between model outcomes and epidemiological data regarding the fraction of vaccinated detected cases is presented in Fig. 4.

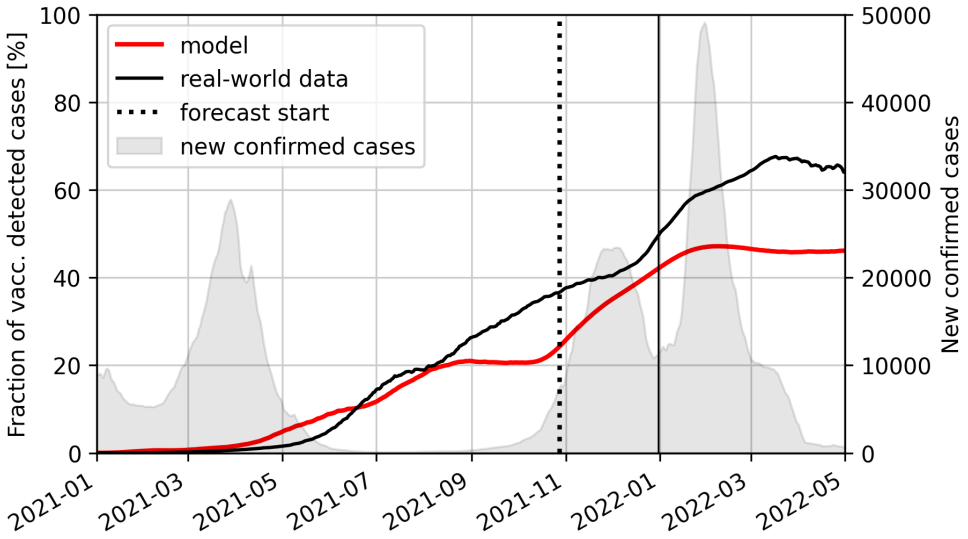

Fig. 4 Comparison between the fraction of vaccinated detected cases generated from the pDyn model (red line) and epidemiological data (black line). The vertical dotted line indicates the simulation date. The solid vertical line marks the end of the estimation period for the quantitative model to real-data fit indices. The transparent grey shape in the background represents the number of new real-data cases.

Generally, the dynamics obtained from the pDyn model converged with the epidemiological data. The mean absolute error from January 1, 2021, to October 28, 2021 (forecast date) equals 3.44%, from October 29, 2021, to December 31, 2021, equals 7.23%, and from January 1, 2022, equals 16.34%. The maximal error from January 1, 2021, to October 28, 2021, equals 14.01%, from October 29, 2021, to December 31, 2021, equals 12.20%, and from January 1, 2022, equals 21.69%. The relatively sizeable maximal error before the forecast date may have resulted from the variation in data when the number of cases was still low while the vaccination uptake reached its saturation point (Fig. 3 green line).

The quantitative indices used to validate the Delta wave forecast were estimated until December 31, 2021, when the Omicron wave officially began. When considering the whole period (from January 1, 2021, until May 1, 2022), the maximal error occurred on March 17, 2022, after the Delta domination period. As the Omicron variant was not considered in the forecast, the highest discrepancy between our simulation and the real-world data was expected to appear after December 31, 2021.

2.2 Predicting the epidemic dynamics during the Delta wave on the national level

In Figs. 5 and 6, we present the forecast for the numbers of new confirmed cases, COVID-19-related deaths, hospitalized patients, and ICU patients during the entire course of the epidemic described in this work (Fig. 5), and Delta-wave alone (Fig. 6), respectively. We assessed model results against real-world data using estimates of the forecast of the peak timing, peak value, and wave length. The results are presented in Tab. 1.

The forecast of the peak value tended to be overestimated and was the most accurate for the new cases (relative difference of $\sim$7%) compared to other metrics. As shown in Figs. 5 and 6, the predicted number of hospitalized patients, ICU patients, and COVID-19-related deaths was higher than official data provided by Ministry of Health: hospitalized patients by $\sim$76%, ICU patients by $\sim$151% and COVID-19-related deaths by $\sim$101%. In terms of the peak timing, our predictions were most accurate for hospitalized patients (2-day difference), followed by reported deaths (4 days), new confirmed cases (6 days), and ICU patients (7 days). The forecast of the wave length measured using the Full-Width Half-Maximum (FWHM) was the most accurate for ICU patients ($\sim$1%) and hospitalized patients ($\sim$8%), followed by reported deaths ($\sim$10%) and new cases ($\sim$51%). A notable relative difference in FWHM between the modeled and observed new confirmed cases was likely due to the holiday period in late December 2021, which resulted in a lower testing rate and detection ratio than before the holidays. As our model assumes a constant detection ratio, the real-life decrease in reporting likely contributed to the discrepancy in the confirmed cases wave length mentioned above.

The model's objective was not to predict the actual number of hospitalized and ICU patients but to estimate their expected number based on the available government data. This distinction should be kept in mind when interpreting the results, as it may account for the significant difference between the model's prediction of the peak value for hospital and ICU beds and the real-world data. Nevertheless, predictions of

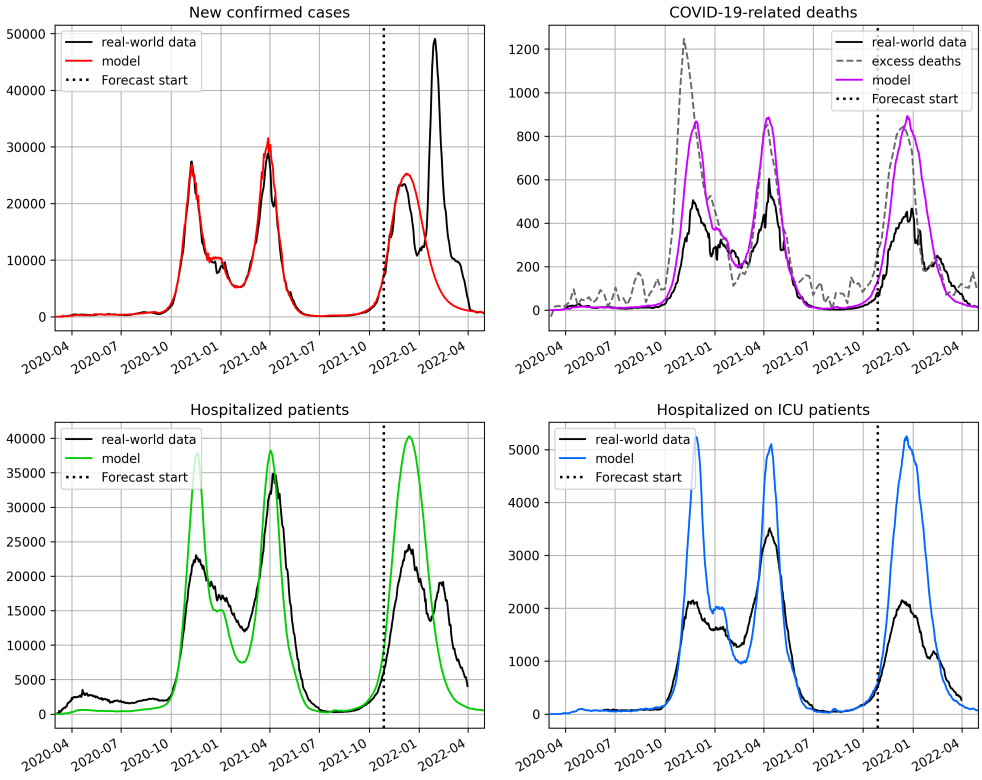

Fig. 5 Comparison between the pDyn model-generated dynamics (colored lines) and the epidemiological data published by the Polish Ministry of Health (black) and Eurostat [31] (dashed grey) for the entire course of the COVID-19 epidemics in Poland. Top left: new confirmed cases. Top right: COVID-19-related deaths. Bottom left: hospitalized patients. Bottom right: ICU patients. The vertical dotted line indicates the simulation date.

peak timing of hospitalized and ICU patients demonstrated that our forecast accurately captured the dynamics of the Delta wave. We used occupied beds instead of hospital admission to assess hospitalizations, as the Ministry of Health only provided hospitalization data about occupied beds. Similarly, we faced the same limitation in assessing ICU hospitalizations.

Additionally, we found excess deaths to be a more reliable parameter than the officially registered COVID-19 deaths. For this reason, we present here the forecast of numbers of COVID-19-related deaths compared to the estimates of excess deaths as defined by Eurostat: *Excess mortality is the rate of additional deaths in a month compared to the average number of deaths in the same month over a baseline period (2016-2019). The higher the value, the more additional deaths have occurred compared to the baseline. A negative value means fewer deaths occurred in a particular month compared with the baseline period* [32]. However, for better quantitative comparison, we provide data in weekly resolution computed using Eurostat weekly data

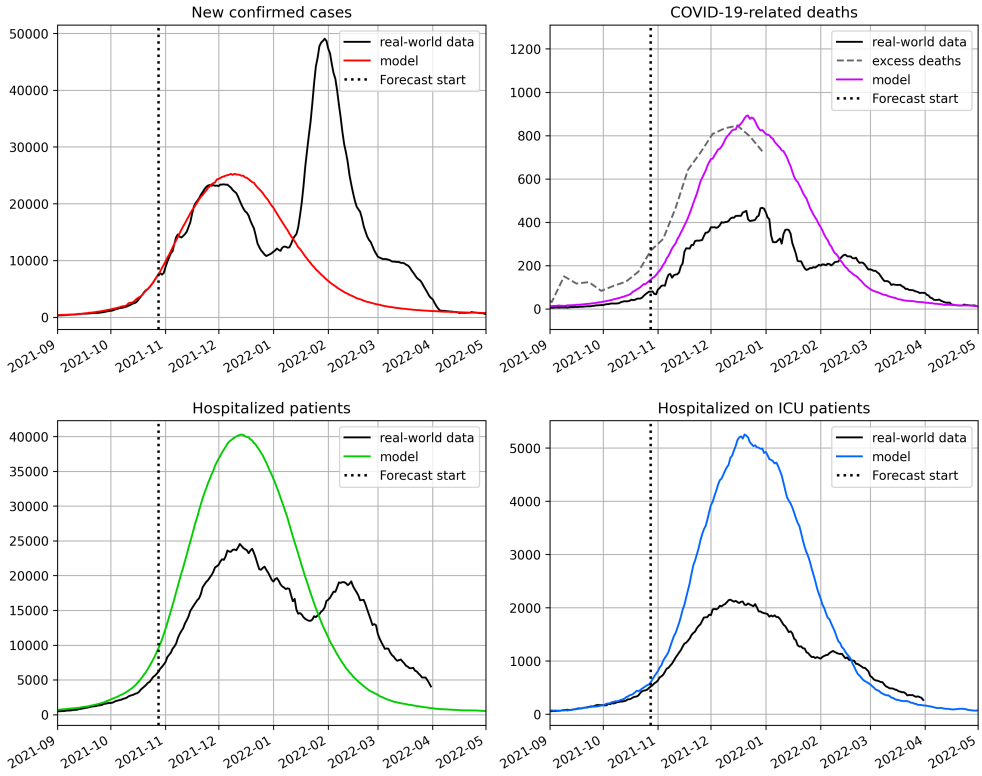

Fig. 6 The zoom into the Delta wave of the COVID-19 epidemics in Poland: comparison between the dynamics generated from the model (colored lines) and the COVID-19 data from the Polish Ministry of Health (black) and Eurostat [31] (dashed grey). Top left: new detected cases. Top right: deaths. Bottom left: hospitalized patients. Bottom right: ICU patients. The vertical dotted line marks the simulation date.

on deaths [31]. The quantitative estimates of the peak timing, peak value, and wave length are presented in the lower panel of Tab. 1. The predicted number of deaths was more following excess deaths than reported deaths in terms of the peak value (relative difference of ∼5% vs. ∼101%) and wave length (∼3% vs. ∼10%).

2.3 Prediction of epidemic dynamics during Delta wave on regional level

Here we demonstrate the ability of the model to forecast epidemic dynamics of disease-related states in voivodships using national-level epidemic data for calibration. The regional trajectories were differentiated due to the synthetic society's spatial structure and vaccination process, regional variation of weight multipliers accounting for differences in NPIs implemented before the Delta wave, and the location of initial infections for each variant introduced into the simulation.

Table 1 The comparison between pDyn simulation results and epidemiological data (see text) for disease-related states regarding the peak value, peak date, and Full-Width Half-Maximum (FWHM) of the Delta wave in Poland is presented. All data is reported daily.

		Peak value	Peak timing	Wave length (FWHM)
New confirmed cases	Simulation	25770	2021-12-05	68
	Real-world	24120	2021-11-29	45
	Difference	1659	6	23
	Relative difference	6.84%		51.11%
Hospitalized	Simulation	41315	2021-12-12	66
	Real-world	23520	2021-12-10	61
	Difference	17795	2	5
	Relative difference	75.66%		8.20%
ICU patients	Simulation	5311	2021-12-21	66
	Real-world	2115	2021-12-14	67
	Difference	3196	7	-1
	Relative difference	151.11%		-1.49%
Reported deaths	Simulation	889	2021-12-21	68
	Real-world	443	2021-12-17	62
	Difference	446	4	6
	Relative difference	100.68%		9.68%
Excess deaths	Simulation	889	2021-12-21	68
	Real-world	845	2021-12-10	66
	Difference	44	11	2
	Relative difference	5.21%		3.03%

The comparison between the data generated from the model and the real-world data over the entire course of the epidemic in voivodships (the total number of detected cases, COVID-19-related hospitalizations, COVID-19-related ICU occupation, and COVID-19-related deaths) are presented in Fig. S6.1-S6.4 in Supplementary. The quantitative comparisons of the peak timing, peak value, and wave length are also included in Supplementary (see Tab. S6.1). Below, in Fig. 7, we present only the summary statistics of model accuracy on the regional level. The top panel of Fig. 7 shows the distributions of peak values, peak dates, and values of FWHM in voivodships obtained from the model (upward distributions) and real-life data (downward distributions). For clarity of presentation, the bottom panel shows the same data as distributions of absolute (for peak date) or relative (peak value, FWHM) differences between model and real-life data.

Medians of difference distributions (marked by the vertical black lines) presented in the bottom panel of Figure 7 roughly follow the differences reported on the national level. In addition, one can see a few outliers in relative peak value difference and FWHM difference graphs for newly detected cases, hospitalized patients, and deaths.

Looking at the distributions of the differences (bottom panel in Figure 7), in particular at relative peak value difference (left plot) in terms of detected cases, occupied beds (hospitalized), and deaths, one can see a clear outlier in each plot, which is Podkarpackie voivodeship. The considerable relative differences observed among voivodeships may be partially attributed to regional behavioral factors, such as a lower willingness to undergo COVID-19 testing or seek hospital treatment for COVID-19than in other parts of the country.

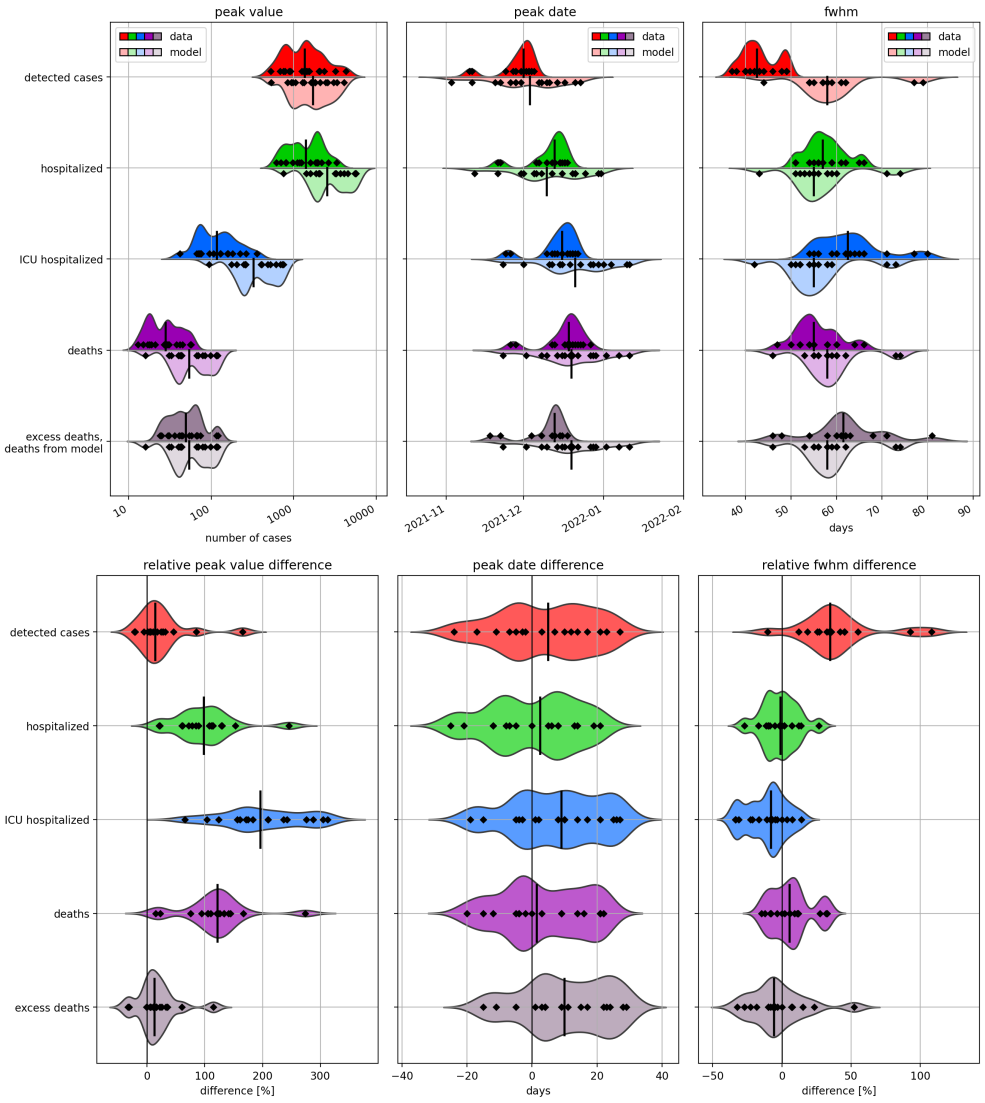

Fig. 7 Summary results for the model forecast on a regional level. Each data point refers to one voivodeship. Upper panels present smoothed distributions of peak value, peak date, and FWHM separately for the Ministry of Health data (at the top of horizontal reference lines) and the model forecast data (at the bottom of the lines) for daily new detected cases, occupied hospital beds, occupied ICU beds, COVID-19 deaths. Additionally, we present the plots for excess deaths based on the Eurostat data [31]. Lower panels present smoothed distributions of relative peak value difference, peak date difference, and relative FWHM difference between the model forecast and the official data. The data points are accompanied by median values (vertical black segments).

On average, the pDyn yields convergence with the real-world data and predicts the number of newly detected cases on the level of single voivodships with similar accuracy to the predictions on the national level.

3 Discussion

Mathematical models of the epidemic are essential to understand its course and can provide information for decision-makers responsible for planning effective mitigation policies [13, 14, 33–35].

In this manuscript, we present validation of implemented epidemic dynamics and assessment of the forecasts accuracy of pDyn, generative ABM tailored to model and predict the dynamics of COVID-19 in Poland.

One of the key features of pDyn is its ability to represent complex social networks and contact patterns among individuals, which significantly impacts the spread of epidemics. Additionally, the model can simulate epidemics at various spatial scales, from small neighborhoods to bigger regions, by incorporating spatial information such as population structure, transportation networks, and geographic features.

Furthermore, pDyn incorporates a model for immunity acquisition and waning, which enables simulation of the effects of vaccination and natural infection. This feature allows for the simulation of the spread of multiple pathogen variants and cross-immunity, facilitating an exploration of the impact of variant and vaccine diversity on epidemic dynamics.

Moreover, pDyn can provide insight into the network-based mechanism of epidemic spread. Unlike phenomenological models, our generative model explores the underlying dynamics driving the spread of the epidemic, including the impact of social networks and individual behavior. Hence, it can simulate the effects of various intervention strategies, such as quarantine and social distancing, on the spread of epidemics, evaluate their effectiveness, and inform public health policies, providing a tool for planning the epidemic response.

The study presented in this manuscript has three specific objectives:

1. To evaluate the validity of dynamics implemented in the model, including the succession of pathogen variants, dynamics of immunization, and the ratio of vaccinated among confirmed cases.
2. To assess the ability of the model to forecast the dynamics of the number of confirmed cases, hospitalizations, ICU hospitalizations, and deaths during the epidemic wave in terms of peak timing, peak value, and wave length.
3. To assess the ability to use pDyn to forecast epidemic dynamics of disease-related states in the highest administrative units in Poland (voivodships) using data reported on the national level, thanks to the virtual society reflecting the social-demographic structure of the Polish population.

In this study, we addressed all these objectives and discussed the results below.

The first variable examined for implementation validity in the model was the succession of the variants. The dynamics of the succession of the variants in the model depends, among other factors, on the pathogen variant properties (cross-immunity, variant infectivity) and the spatiotemporal distribution of initial infection for each variant.

In our study, we found that the Delta variant reached a prevalence of 25%, 50%, and 75% 2, 3, and 4 weeks later, respectively, compared to the GISAID genomic data. Our validation is in line with previous studies such as [36] and [37], which also

compared the succession of variants at the 50% prevalence point. In those studies, the prediction errors were within one week, two weeks, and one week, respectively, indicating that the accuracy of the results was similar, albeit slightly better than our pDyn model. However, the better performance of other models compared to pDyn is likely due to calibration and validation on the same datasets. In contrast, pDyn was calibrated and validated on two separate datasets. Furthermore, two other studies presented only visual comparisons [38, 39]. Also, the GISAID estimates for Poland may suffer from selection bias, which could contribute to the differences. Conclusively, our results demonstrate that pDyn produces a realistic succession of variants.

We then compared our modeling results with the OBSER-CO seroprevalence survey conducted by the National Institute of Public Health. Our model's cumulative number of recovered and vaccinated individuals matched the seroprevalence study's estimates at all four timepoints. However, the estimate from the model for the December 2021 time point was too high, falling 3 pp outside the 95% confidence interval. While models similar to ours have been calibrated against seroprevalence data, to our knowledge, they have not yet been validated against them [40, 41].

It is worth noting that a non-matching data point was after the forecast date, so assessing the accuracy of the dynamics implemented before the forecast is not strictly appropriate. Additionally, the OBSER-CO results may be imprecise due to the bias in seropositivity estimates caused by examinations being taken when the number of detected cases was unstable [42]. Also, the study rounds were extended over time, with unevenly distributed testing within each round, while seroprevalence was estimated just at central time points of each round interval, which may have further affected the accuracy of the estimates. Moreover, the sum of recovered and vaccinated cases derived from the model does not perfectly correspond to OBSER-CO seroprevalence statistics based on antibody levels in the trial groups. However, despite these reservations, pDyn's representations of immunity in society closely reflect empirical OBSER-CO studies. Finally, to our knowledge, pDyn is the first model that accurately reflects the empirical OBSER-CO studies, making it a valuable tool for exploring the dynamics of epidemics.

The proportion of vaccinated detected cases that emerged as a simulation variable was compared with surveillance data provided by the Ministry of Health. We used mean absolute error as the validation metric. Before the forecast date, the mean absolute error was smaller than in the forecast period, reflecting the uncertainty of the prognosis. Also, the maximal absolute error occurred on October 18, 2021, at 14.01 pp., likely when the number of cases remained low while vaccination uptake reached its saturation point. To our knowledge, the proportion of fully vaccinated among detected cases has been used to assess vaccine effectiveness [43], but not in modeling epidemics. It is worth noting that empirical data regarding the fraction of vaccinated detected cases were only available after predictions were made, making model calibration using this data impossible.

In summary, the pDyn model generated dynamics that generally aligned with epidemiological data. The convergence between the model results and real-world data confirmed the validity of the dynamics implemented in the model concerning variant succession, immunization, and the emergence of vaccinated among confirmed cases.

The proposed new method of handling uncertainty in generative models presents an additional value to modeling studies in epidemiology. ABMs typically have numerous parameters that need calibration, and often, the available data are insufficient for calibrating each parameter. In such situations, a part of the model validation should involve comparing variables that are not direct outputs from the model but can be obtained from the model and compared to existing data before making the forecast (e.g., the dynamics of pathogen variant succession). This process helps confirm the validity of the epidemiological dynamics implemented in the model without needing to validate model parameters individually.

In the second part of the results, we evaluated the accuracy of forecasts for the fourth wave, driven by the Delta variant, at the national level concerning new cases, hospitalizations, ICU admissions, and COVID-19-related deaths. We assessed the validity of each disease-related state by examining peak value, peak date, and wave length.

Our assessment of forecasting initially focused on new COVID-19 cases, which served as the primary calibration reference. We achieved accurate forecasts for the peak value of new cases. Predictions for new cases were more precise (with a 6.84% difference) than for other states, for which overestimations were common. However, the peak timing forecast for new cases was delayed by six days. Additionally, wave length prediction (using FWHM) was the least accurate for new cases, partially attributed to the holiday season in December 2021. During this time, testing rates and detection ratios decreased, resulting in fewer confirmed cases. As our model assumes constant detection ratios, this decline in reporting may partially explain the discrepancy between modeled and observed wave lengths for confirmed cases.

The model predicted a significantly higher number of COVID-19-related general and ICU hospitalizations than the Ministry of Health reported, with 76% more hospitalizations and 151% more ICU patients. We focused on required instead of occupied beds, assuming that even if some patients needing hospitalization stayed home, the health system should be prepared. Consequently, the model assumes constant hospitalization durations of 10 days for general and seven days for ICU admissions instead of using distributions. This assumption is a primary source of the discrepancy between the model and data. Additionally, poor data quality related to hospitalization durations adds uncertainty to estimations.

Our analysis revealed dynamically changing case-to-hospitalization and case-to-death ratios throughout the waves. These changes can be attributed to social reluctance towards testing and hospitalization due to difficult hospital conditions. Factors such as lack of family contact, admission challenges, and long queues at testing sites contributed to this reluctance [44–49]. However, the model did not account for psychological and healthcare system overload effects, which also affected the accuracy of our target variables.

Despite these caveats, peak time forecasts for hospitalizations were the most accurate among predicted disease-related states (2 days delay), and the relative wave length difference was best for ICU patients (-1.5%). In summary, the discrepancy between hospitalization and ICU patient data and model results can be attributed to various factors, mainly related to wave magnitude rather than peak or length. This result

highlights the importance of considering data collection and nowcasting issues when interpreting modeling results [50–52].

In this study, pDyn predicted more COVID-19-related deaths than reported. Excess deaths proved to be a more reliable parameter for capturing the actual number of deaths than the officially registered COVID-19 deaths, consistent with evidence suggesting a significant number of undetected infections. For instance, Walkowiak [53] found that combined COVID-19-related deaths accounted for 95% of excess deaths among Polish adults over 40. Death forecasts closely aligned with excess deaths in peak value (5% relative difference) and wave length (3% relative difference). However, the peak date forecast for deaths was the least accurate among all forecast states, with an 11-day delay.

In conclusion, our simulation and forecast converged with epidemiological data for new cases, COVID-19-related deaths, hospitalizations, and ICU patients at the national level.

The pDyn model was based on a synthetic society closely aligned with regional socio-demographic data. It explicitly accounted for regional differences in vaccination, pre-Delta wave NPIs, and the regional distribution of initial wild-type infections in Poland. However, its calibration relied on national epidemic data. Our next goal was to assess the accuracy of regional forecasts from this model, focusing on individual voivodeships.

Our study results indicate that, on average, regional forecasts align with national-level ones. Specifically, the medians of difference distributions tend to follow the differences reported at the national level. However, prediction quality varies among voivodeships. Notably, Podkarpackie voivodeship is a clear outlier in relative peak value differences for detected cases, occupied hospital beds, and deaths. Significant relative differences between predicted and observed peak values among voivodships are likely due to local variations in social reactions to the epidemic and restrictions. This result suggests that for regional forecasting, enhancing model performance requires accounting for regional variation in social attitudes. Generally, to achieve greater prediction accuracy at the regional level, incorporating more agent features related to behavioral characteristics, such as trust in medicine, willingness to comply with NPIs and vaccination acceptance, is recommended.

In conclusion, our study demonstrates the capabilities and potential of the pDyn model to provide reliable and insightful forecasts for various aspects of the COVID-19 pandemic. The key findings in our research can be summarized as follows:

- Due to a meticulous generative description of the epidemic spread, the pDyn model achieves remarkable performance in predicting cases, hospitalizations, ICU hospitalizations, and deaths, as assessed by German and Polish COVID-19 Forecast Hub [24, 25] and European COVID-19 Forecast Hub [54].
- Our generative ABM benefits from complex internal states, enabling the implementation of mechanisms that phenomenological models cannot capture and allowing the incorporation of vast amounts of data. Moreover, complex internal states of the model increase its accuracy and provide unique insights into ongoing epidemiological processes.

- We propose a new method to deal with uncertainty in generative models by comparing variables that are not direct outputs from the model but can be obtained and compared to existing data before making forecasts. This validation can contribute to analyzing patterns reproduced by the model [10].
- The pDyn model allows for detailed epidemic simulation in Polish society at national and regional levels, although forecasting at the regional level based on national data has some limitations. Additionally, the network structure enables excellent modeling resolution down to specific agents or contexts, allowing for modeling NPIs and various scenarios.

Despite the promising results, our study has certain limitations. For instance, the accuracy of regional forecasts varies between voivodeships, suggesting that incorporating more agent features related to behavioral characteristics might improve regional prediction accuracy. In addition, data availability remains a fundamental limitation of the pDyn model. Some crucial datasets were unavailable at our forecast (e.g., contact tracing data, an influx of new cases, the number of households in quarantine, and estimated transmissions between household members). This conclusion also highlights the importance of robust epidemic surveillance systems for the mathematical modeling of epidemics.

Nevertheless, even in conditions of limited data availability, the pDyn model enabled an insightful description of processes and remarkable forecasting efficiency. Therefore, the model can help in understanding the mechanisms of the epidemic and designing epidemic policies, including comparing multiple scenarios.

In terms of future work, we plan to focus on integrating and consolidating datasets to improve the model's accuracy and robustness. The model can also help determine the optimal set of data that should be collected during an outbreak, which is an area we will investigate in our future research. This approach will not only enhance the model's predictive capabilities but also guide data collection priorities in future epidemics, contributing to more effective and targeted public health responses.

4 Methods

4.1 The pDyn model

Our research utilizes pDyn, the detailed epidemiological ABM developed at the Interdisciplinary Center for Mathematical and Computational Modelling at the University of Warsaw, Poland (ICM) [18]. The simulator was optimized for High-Performance Computing environment and runs in the ICM supercomputing facility.

The model originated as designed to simulate the influenza epidemic [17]. Subsequently, during the COVID-19 pandemic, it has been expanded with features tailored to represent characteristics of the SARS-CoV-2 infection, to facilitate the Polish government's infection prevention and control the decision-making process.

To better illustrate the pDyn's scale and complexity, we present a mind map (Fig. 8) that organizes the model elements in a clearer, modular way. The figure illustrates the version of the model used in the study. Functions developed by adapting the original version of the simulator to the COVID-19 are marked in the figure by

asterisk. The detailed description of the pDyn model following the Overview, the Design concepts, and the Details protocol (ODD, [55]) is publicly available [18].

Fig. 8 Mind map of the features of the current version of pDyn model. The model has 4 classes of features: (1) describing the nature and effects of the pathogen (in our study, SARS-CoV-2), (2) contact structure describing the demography and mobility in the given area (in our study, Poland), (3) effects of pharmaceutical and non-pharmaceutical mitigation policies, and (4) regulating the consistency between the model and the real-world data. Most of the components are new (marked by asterisk) in comparison to original model version.

The overall *purpose* of the pDyn model is to describe and explain the spatial and temporal dynamics of SARS-CoV-2 spread across Polish society. The model predicts the dynamics of the number and locations of disease-related states of agents in response to specific changes in the properties of the pathogen and the social structure and behaviour.

Two types of *entities* are included in the model: agents and contexts. Agents represent members of the society. Contexts capture interactions between agents; they represent locations at which the agents come in contact, such as households, workplaces, kindergartens, schools, universities or public places. Their geo-localized representations are included in the synthetic society as model input [16]. The synthetic society is based on data provided by the Statistics Poland [56] and reflects the state at the beginning of 2019. The *spatial resolution* of the contexts is a grid of 1×1 km^2 (for Poland, it requires 800×800 grid cells). Additionally, pDyn models the mobility of agents via random long-distance travels (i.e. when an agent leaves its household for more than a day). Each agent is assigned to one or more contexts (household at least) that it visits daily.

Both agents and contexts are characterized by *state variables*. The agent's state variables are as follows: age, list of contexts to which it is assigned (including primary household), disease-related state, presence of symptoms, being on quarantine, travel status, transmission location, and history of immunization events. The context's state variables are as follows: spatial coordinates of a given context, transmission rate in this context, the number of agents in this context, the number of symptomatic infectious agents in this context, and the number of non-symptomatic infectious agents in this context. The *time resolution* in the simulation is one day.

The most important *process* of the model is airborne transmission.

For a given susceptible agent, for a given day of the simulation, and a given variant of the virus, the probability of becoming infected by that variant on the following day is computed based on three factors: (1) the infectivity parameter specific to the variant, (2) the infectivity of the contexts visited during the day which we define as the fraction of infectious agents infected with the considered variant in that context, (3) the weights of the daily visited contexts which represent the contact rate of the agents in that context.

Thus, the probability of each susceptible agent getting infected on the next day of the simulation is a function of the *disease-related states* of all agents with whom it has been in contact in contexts during the current day [18]. Immediately after the recovery or after taking a vaccine, the agent is immune to the infection variant of the pathogen, but the level of immunity wanes over time. The level of immunity calculated on a given day of the simulation modifies the probability of infection with the variant. In addition, recovery from infection with a particular variant of the virus generates a certain level of cross-immunity to other variants. Furthermore, the context weights are adjusted using *multipliers* in time to represent the changes in the contact rates (i.e., the number of contacts made divided by the number of contact opportunities) due to behavioural reactions to the epidemic, both spontaneous or in response to the control measures.

The model of possible *disease-related states* in pDyn expands the SEIR (Susceptible, Exposed, Infected, Recovered) compartmental model [57]. An agent can find itself in one of the following disease-related states: susceptible, latent, asymptomatic, symptomatic, hospitalized outside the ICU, hospitalized before ICU, hospitalized at ICU, dead, or recovered state. These disease-related states form an ordered graph that

defines possible courses of infection (Figure 9). At each branching, probability parameters have been introduced to control the likelihood of the specific transitions between states (specific to the pathogen variant).

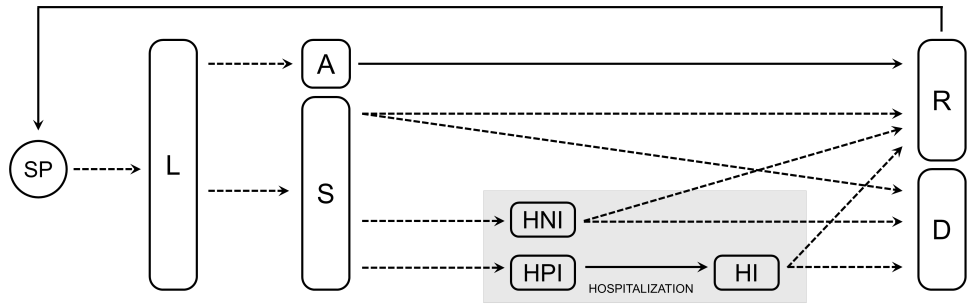

Fig. 9 The possible paths through disease-related states in the pDyn model. The state abbreviations stand for SP — susceptible, L — latent, A — asymptomatic, S — symptomatic, HPI — hospitalized, pre-ICU, HI — hospitalized, at ICU, HNI — hospitalized, not at ICU, D — dead, R — recovered. In addition, there are three surefire paths (with transition probability equal to 1; marked with solid arrows) regardless of the agent's age.

In addition, the duration of each state is defined. The transition probabilities and the duration of states depend on agent's age. It is assumed that both the asymptomatic and symptomatic states are infectious and that infectivity in the symptomatic state is higher than in the asymptomatic one [58–60]. On the other hand, there is a possibility for an agent in a symptomatic state to undergo self-isolation or quarantine, meaning the agent withdraws from all contexts except for the household. The probability and duration parameters were selected based on several studies [61–65] and their values implemented in the present simulation are presented in Tables S3.4 and S3.5 in Supplementary Material.

In the pDyn, the number of infected agents includes both detected and undetected cases. Undetected cases impact various aspects of pandemic dynamic such as the true disease spread, the number of immunised individuals, numbers of hospitalized cases and deaths. The model introduces a *dark figure* representing the number of undetected cases, generating outputs for both real cases (detected and undetected) and detected cases. The dark figure changes over time and is estimated by considering factors such as the ratio of non-symptomatic to symptomatic cases, testing strategies, test types, test numbers, contact tracing, public trust, and seroprevalence screening studies [66].

The pDyn model allows for simulating vaccination programs, considering factors like geographical distribution, agent's age, and the number of vaccines administered. However, the presented simulation is agnostic to the type of vaccination, treating boost vaccinations the same as first doses, and not differentiating between various vaccines. The model offers fine-tuned control of vaccination, allowing for region-specific and age-based vaccination strategies with limited supply considerations based on data based

on data provided by Polish government under the license defined in a Non-Disclosure Agreement.

The pDyn allows to explicitly model addresses the cross-immunity phenomenon. The model assumes that the agent is immune to the infection variant immediately after recovery or after taking a vaccine, albeit the immunity level is waning over time. The decline in the immunity level is described in the function of elapsed time since recovery and can take values between 0 and 1 (See Figure S3.1). The immunity level of an agent computed on a given day of the simulation modifies the probability of infection with the variant subject to immunity. Moreover, we model the phenomenon of cross-immunity by assuming that recovery from an infection with a specific virus variant generates some immunity level to other variants. The parameters related to (cross-)immunity were estimated from [67] and presented in Table S3.2.

The pDyn allows to model risk exposure changes, whether seasonal (e.g. school closure during holidays) or behavioural (e.g. in response to NPIs, e.g., online schooling), by switching off or tuning contexts, using context weight *multipliers*. To our best knowledge, no systematic studies of contact rates changes were carried out during the COVID-19 epidemic in Poland. Instead, the models use intermediate (e.g., estimates based on measurements of the use of mobile networks) or partial (e.g., social mixing surveys) measures. In pDyn, the initial contacting rates were adopted from original influenza model [17]. Changes in contact rates during the outbreak and subsequent restrictions were implemented through multipliers.

In order to model changes in the contact rate for a particular context, we utilized the calibration experiments method, except for educational units, for which these multipliers were estimated based on the proportion of pupils attending them. Multipliers for the households, workplaces, and public places were adjusted with an assessment of the change in contact rates (based on changes in the number of people and their compliance with social distancing measures in a given context). The calibration experiments were executed in the following way: first we established the optimistic and pessimistic contact rate scenarios by assessing the minimum and maximum values of multipliers (such as low vs. high face mask use compliance). For example, on March 12, 2022, the mandate of remote work and social distancing at the workplace was introduced, therefore we reduced the value of the workplace context multiplier from 1 to 0.5 in the optimistic scenario and to 0.8 in the pessimistic scenario. Then, we tested several multiplier values in the selected range to compare the results with the actual data of the identified cases from 14 days after the introduced change and adjusted the value of multipliers as necessary. In order to determine the best set of multipliers, the Fréchet distance between the number of confirmed cases predicted by the model and the real-world data was minimized. The final list of all context multipliers is presented in Table S3.6 in the Supplementary Material.

Regional diversity of the predicted epidemic dynamic on voivodship level is only due to a spatial structure of the synthetic society, some regional differentiation of weight multipliers motivated by regional NPIs in force before the Delta wave as well as location of infected agents spatially placed at the simulation date.

4.2 Input data and calibration

In pDyn, the infection spread is simulated on a synthetic representation of Polish society comprising about 38 million agents representing Poland's population in 2019, simulated based on Statistics Poland data, both publicly [16, 56] and not publicly available. Non-public data was provided under the license defined in a Non-Disclosure Agreement and can be made available with the permission of the data provider. The spread of epidemics and individual virus variants begins with initial infections, which serve as an initial condition of the simulation. Data on the date and location of the initial infections have provided by the Polish Ministry of Health (please see Table S2.1 containing data sources). Initial parameters are loaded together with the synthetic society at the beginning of the simulation. The initial parameters include pathogen properties (infectivity, probabilities and times of disease-related states per variant), the proportion of undetected cases, quarantine probability, cross-immunity and immunity waning parameters, and context weights, and their multipliers.

Two parameters, namely the basic pathogen variant infectivity (α) and the fraction of not self-isolating symptomatic agents (f) were fitted in the model calibration process using Bayesian optimization [68] to the real-world number of confirmed cases provided initially by Michał Rogalski and then by the Polish Ministry of Health (please see Table S2.1 containing data sources). The remaining parameters were taken from the literature (as indicated in the model description) or estimated based on calibration experiments, such as those described for modeling changes in the contact rates for different contexts (*multipliers*). Similarly to setting optimistic and pessimistic scenarios for multipliers, we dealt with the uncertainty for the remaining model parameters by setting specific prediction intervals based on optimistic and pessimistic scenarios.

In stochastic models, such prediction intervals may arise from several interrelated sources. Firstly, it can be derived from a number of simulations carried out with alternating seeds of the pseudo-random number generator. Secondly, it can be derived from several simulations with alternating input parameter values taken from appropriate distributions. Thirdly, the assumed or prepared initial state of the system, e.g. the immunisation of the population, might strongly affect the outcome values of the simulation. Finally, the result of time-dependent curve prediction intervals for each time point forms a confidence interval.

As a result, broad prediction intervals can be obtained in the simulations of highly non-linear systems, where the small random change of input parameters might result in a significant output change. However, the broad prediction intervals appear when input parameters are delivered with a broad range of possible values or where the system's initial state features are largely unknown. In our case, the nonlinearity of the model is limited, and the main source of the output uncertainty comes from the uncertainty of various parameter values and the system's initial state. In such a situation, apart from computing the confidence corridors resulting from the randomness of the process, the two extreme scenarios have been formulated: the lowest (optimistic) and the highest (pessimistic), regarding possible but still realistic values of parameters and initial states of the system. The two scenarios determine the prediction interval for our forecast. The contrast in uncertainty coming from different sources (random

seed vs two scenarios) is illustrated for the simulation described in this article and is in Supplementary Material S4.

4.3 Simulation setup

4.3.1 Model calibration

The simulation used in this study was conducted on October 28, 2021. In order to account for the uncertainty, we have formulated pessimistic and optimistic scenarios differing in the dark figure parameter (see Supplementary Material S4. The pessimistic scenario proved to yield a more accurate prediction of the Delta-variant wave than the optimistic scenario. Therefore, all presented results come from the pessimistic scenario).

4.3.2 Testing validity of the model dynamics

It should be noted at the beginning that when testing the validity of the model, we compared the real-world data (other than those to which we calibrated the model) to our model estimates to evaluate whether the pDyn reproduced the dynamics of the epidemic accurately up to the time of simulation (i.e., October 28 2021). When testing the accuracy of the pDyn's predictions, we retrospectively compared the results obtained in the simulation with real-world data acquired after the simulation date to evaluate pDynas a tool for predicting the future epidemic spread.

We tested the validity of the epidemic dynamics implemented in the model by comparing our simulations with real-world data regarding the dominating SARS-CoV-2 variant, immunization level in the population, and the fraction of vaccinated amongst detected cases.

The emergence of the variants of pathogen in the real world is monitored, and data are collected and accessible via Global Initiative on Sharing Avian Influenza Data (GISAID) portal [29]. The distribution of SARS-CoV-2 variants in our model was validated by comparison with the genomic data from the GISAID. Before the day of our simulation, three dominant variants have been detected in Poland (namely, the wild type, Alpha, and Delta). To account for the possible low representativeness of the GISAID samples available for Poland, we assessed whether the curves representing the temporal succession of the wild type, Alpha and Delta variants obtained from our model mirrors the analogous "succession curves" obtained from GISAID by comparing the time convergence of reaching 25%, 50%, and 75% prevalence for each variant.

Similarly, to establish the immunization level (the fraction of agents who have been vaccinated or have undergone disease and are still immune), we compared the model results with the results of a nation-wide seroprevalence survey of adults aged 19 years and older (named OBSER-CO) run by the National Institute for Public Health in Poland [30, 66]. This data was collected in four rounds (I round: 29 March to 14 May 2021, II round: 27 July to 10 September 2021, III round: 16 November to 23 December 2021, IV round: 14 March to 4 May 2022) alongside with 95% confidence intervals for each estimate. The OBSER-CO seroprevalence estimates were used to approximate the validity of pDyn's predictions of the cumulative sum of recovered and vaccinated

agents. As only the adult population was studied in the OBSER-CO study, data of agents younger than 19 years were not included in Fig. 3.

Lastly, using the Ministry of Health data on the age, time, and location distribution of vaccinations, pDyn model computed the fraction of vaccinated among the detected cases. We tested the validity of this estimate by comparing it with the Ministry of Health's estimate of the fraction of vaccinated detected cases in the population using mean absolute error (MAE) method.

4.3.3 Testing the forecast accuracy

In order to evaluate the performance of our model and the accuracy of the simulation in reproducing the COVID-19 dynamics, we compared its results to real-world data (from the Ministry of Health [quote]) using three key measures of discrepancy: (1) the difference in peak date, (2) the difference in peak value, and (3) the difference in wave length.

To calculate the differences, we first characterized the peaks of the COVID-19 pandemic by fitting a parameterized analytical function to the data indicating the occurrence of a wave. As the logistic curve is typically used to approximate a cumulative number of infected cases in epidemics [69, 70], its derivative, known as the logistic distribution, is a natural choice for a description of daily cases. The logistic distribution is parameterized by three quantities, which can be matched to our measures: (1) the mean (peak data, the central point of the wave peak), (2) the height (peak value), and (3) the width (wave length). The latter was adapted for our analysis as a full width at half-maximum (FWHM) [71]. In Supplementary Materials S5 we provided a mathematical formula for calculating FWHM, as well as details and examples of the fitting procedure.

This analysis was applied to the peaks of new confirmed cases, COVID-19-related deaths, hospitalized patients, and ICU patients, both at the national and regional levels, and both for model results and real-world data. Although within the real-world data the Delta wave peaks are usually partially overlapped with arising Omicron wave peaks (not taken into account in the forecast), a sum of two logistic distributions of individual parameters were fitted in this case, and only the first peak of Delta wave was taken for further analysis.

The same method was employed to test the accuracy of predictions at the level of voivodships, which are the basic administrative units in Poland where epidemic data is collected and potential NPIs are introduced.

Supplementary information. Article has accompanying supplementary file: `Supplementary.pdf`.

Acknowledgments. This research was carried out with the support of the Interdisciplinary Centre for Mathematical and Computational Modelling University of Warsaw (ICM UW) under computational allocation no GS80-31.

Declarations

Funding. The present study was a part of the "ICM Epidemiological Model Development" project, funded by the Ministry of Science and Higher Education of Poland with grants 51/WFSN/2020, 28/WFSN/2021, and 37/WFSN/2022 awarded to the University of Warsaw.

Conflict of interest/Competing interests. The authors declare that they have no conflict of interest.

Contributions. Conceptualization - FR, KN, JMN, NB, RPB. Data Curation - AK, MGS, JH. Formal Analysis - FR, MR, KN, JH, DB, JK, BK. Funding Acquisition - FR, AK. Investigation - JMN, FR, KN, MGS, DB, MR, JZ. Methodology - RPB, JMN, FR, JK, GD. Project Administration - FR. Resources - AK. Software - AM, FD,BK, MR, KN, MGS, JK, FD, ŁG, MS. Supervision - RPB, FR. Validation - FR, MR, GD. Visualization - AM, BK, MR, KN, JK. Writing – Original Draft Prep - RPB, JMN, KN, MR, JH, JK, GD, BK. Writing – Review and Editing - RPB, UT, NB, JMN, FR, KN, MGS.

Ethics approval. Not applicable.

Consent to participate. Not applicable.

Consent for publication. Not applicable.

Availability of data. The research presented in this paper is based on both publicly available data and data obtained through an agreement that includes a non-disclosure agreement (NDA). The sources of the data are specified in the Supplementary materials section **??**.

We have taken all necessary measures to ensure the protection and confidentiality of the data used in this study. We recognize the importance of data sharing for scientific progress and are committed to making our data sets available to other researchers upon request, while adhering to any constraints imposed by the NDA.

All publicly available data used in this article is available in the public repository from the link: https://doi.org/10.18150/8XITKG

Code availability. The code used in this research is available at https://git.icm.edu.pl/covid19/data-for-the-article-a-deep-dive-into-the-delta-wave-forecasting-sars-cov-2-epidemic-dynamic-in-polar

References

[1] Ministerstwo Zdrowia. Pierwszy przypadek koronawirusa w Polsce [The first coronavirus case in Poland] (2020). URL https://www.gov.pl/web/zdrowie/pierwszy-przypadek-koronawirusa-w-polsce.

[2] Pinkas, J. *et al.* Public health interventions to mitigate early spread of SARS-CoV-2 in Poland. *Medical Science Monitor* **26** (2020).

[3] Duszyński, J. *et al.* Kroniki pandemii lata 2020-2021 [Chronicles of the 2020-2021 pandemic]. *Academia — Magazyn Polskiej Akademii Nauk* **4**, 1–118 (2021).

[4] Haischer, M. H. *et al.* Who is wearing a mask? Gender-, age-, and address-related differences during the COVID-19 pandemic. *PLOS ONE* **15** (2020).

[5] Delussu, F., Tizzoni, M. & Gauvin, L. Evidence of pandemic fatigue associated with stricter tiered COVID-19 restrictions. *PLOS Digital Health* **1** (2022).

[6] Fox, J. P., Elveback, L., Scott, W., Gatewood, L. & Ackerman, E. Herd immunity: Basic concept and relevance to public health immunization practices. *American Journal of Epidemiology* **94**, 179–189 (1971).

[7] Elveback, L. R. *et al.* An influenza simulation model for immunization studies. *American Journal of Epidemiology* **103**, 152–165 (1976).

[8] Dilaver, O. & Gilbert, N. Unpacking a black box: A conceptual anatomy framework for agent-based social simulation models. *Journal of Artificial Societies and Social Simulation* **26**, 4 (2023).

[9] Epstein, J. M. Agent-based computational models and generative social science. *Complexity* **4**, 41–60 (1999).

[10] Millington, J. D., O'Sullivan, D. & Perry, G. L. Model histories: Narrative explanation in generative simulation modelling. *Geoforum* **43**, 1025–1034 (2012).

[11] Banks, D. L. & Hooten, M. B. Statistical challenges in agent-based modeling. *The American Statistician* **75**, 235–242 (2021).

[12] Silverman, E. *et al.* Situating agent-based modelling in population health research. *Emerging Themes in Epidemiology* **18**, 10 (2021).

[13] Ferguson, N. M. *et al.* Strategies for containing an emerging influenza pandemic in Southeast Asia. *Nature* **437**, 209–214 (2005).

[14] Ferguson, N. *et al.* Report 9: Impact of non-pharmaceutical interventions (NPIs) to reduce COVID19 mortality and healthcare demand (2020). Report at https://doi.org/10.25561/77482.

[15] Pueyo, T. Coronavirus: The hammer and the dance (2020). URL https://tomaspueyo.medium.com/coronavirus-the-hammer-and-the-dance-be9337092b56.

[16] Rakowski, F., Gruziel, M., Krych, M. & Radomski, J. P. Large scale daily contacts and mobility model - an individual-based countrywide simulation study for Poland. *Journal of Artificial Societies and Social Simulation* **13**, 13 (2010).

[17] Rakowski, F., Gruziel, M., Bieniasz-Krzywiec, Ł. & Radomski, J. P. Influenza epidemic spread simulation for Poland — a large scale, individual based model study. *Physica A: Statistical Mechanics and its Applications* **389**, 3149–3165 (2010).

[18] Niedzielewski, K. *et al.* The overview, design concepts and details protocol of ICM epidemiological model (PDYN 1.5) (2022). Preprint at https://doi.org/10.2139/ssrn.4039054.

[19] Adamik, B. *et al.* Mitigation and herd immunity strategy for COVID-19 is likely to fail (2020). Preprint at https://www.medrxiv.org/content/10.1101/2020.03.25.20043109v2.

[20] Pałka, P. *et al.* Using multiagent modeling to forecast the spatiotemporal development of the COVID-19 pandemic in Poland. *Scientific Reports* **12**, 11314 (2022).

[21] Regulski, P., Wendykier, P., Kantiem, K. & Murdzek, W. Advanced methods of visual analysis and visualization of various aspects of the COVID-19 outbreak in Poland. *Procedia Computer Science* **192**, 4194–4199 (2021).

[22] Lorig, F., Johansson, E. & Davidsson, P. Agent-based social simulation of the covid-19 pandemic: A systematic review. *Journal of Artificial Societies and Social Simulation* **24**, 5 (2021).

[23] Ramakrishna, S., Górski, Ł. & Paschke, A. A dialogue between a lawyer and computer scientist: The evaluation of knowledge transformation from legal text to computer-readable format. *Applied Artificial Intelligence* **30**, 216–232 (2016).

[24] Bracher, J. *et al.* A pre-registered short-term forecasting study of COVID-19 in Germany and Poland during the second wave. *Nature Communications* **12**, 5173 (2021).

[25] Bracher, J. *et al.* National and subnational short-term forecasting of COVID-19 in Germany and Poland during early 2021. *Communications Medicine* **2**, 136 (2022).

[26] Frias-Martinez, E., Williamson, G. & Frias-Martinez, V. *An agent-based model of epidemic spread using human mobility and social network information*, 57–64 (IEEE, Boston, MA, 2011). Preprint at https://doi.org/10.1109/PASSAT/SocialCom.2011.142.

[27] Macal, C. M. Everything you need to know about agent-based modelling and simulation. *Journal of Simulation* **10**, 144–156 (2016).

[28] Ritchie, H. *et al.* Coronavirus pandemic (COVID-19) (2020). URL https://ourworldindata.org/coronavirus.

[29] Khare, S. *et al.* GISAID's role in pandemic response. *China CDC Weekly* **3**, 1049–1051 (2021).

[30] National Institute of Public Health. Ogólnopolskie badanie seroepidemiologiczne COVID-19 OBSER-CO podsumowanie wyników II tury badania [nationwide seroepidemiological study COVID -19 OBSER-CO. summary of the results of the 2nd round of the study] (2021). URL https://www.pzh.gov.pl/download/28465/.

[31] Eurostat. Deaths by week and sex (2023). URL https://ec.europa.eu/eurostat/databrowser/product/view/DEMO_R_MWK_TS?lang=en.

[32] Eurostat. Excess mortality - statistics (2023). URL https://ec.europa.eu/eurostat/statistics-explained/index.php?title=Excess_mortality_-_statistics.

[33] Brauer, F. in *Compartmental models in epidemiology* (eds Brauer, F., van den Driessche, P. & Wu, J.) *Mathematical Epidemiology*, Vol. 1945 19–79 (Springer, Berlin, 2008).

[34] James, L. P., Salomon, J. A., Buckee, C. O. & Menzies, N. A. The use and misuse of mathematical modeling for infectious disease policymaking: Lessons for the COVID-19 pandemic. *Medical Decision Making* **41**, 379–385 (2021).

[35] Marshall, B. D. in *Agent-based modeling* (eds El-Sayed, A. M. & Galea, S.) *Systems science and population health* 87–98 (Oxford University Press, New York, 2017).

[36] Eales, O. *et al.* Dynamics of competing SARS-CoV-2 variants during the Omicron epidemic in England. *Nature Communications* **13**, 4375 (2022).

[37] Dong, R., Hu, T., Zhang, Y., Li, Y. & Zhou, X.-H. Assessing the transmissibility of the new SARS-CoV-2 variants: From Delta to Omicron. *Vaccines* **10**, 496 (2022).

[38] Coutinho, R. M. *et al.* Model-based estimation of transmissibility and reinfection of SARS-CoV-2 P.1 variant. *Communications Medicine* **1**, 1–8 (2021).

[39] Campbell, F. *et al.* Increased transmissibility and global spread of SARS-CoV-2 variants of concern as at june 2021. *Eurosurveillance* **26** (2021).

[40] Kemp, F. *et al.* Modelling COVID-19 dynamics and potential for herd immunity by vaccination in Austria, Luxembourg and Sweden. *Journal of Theoretical Biology* **530**, 110874 (2021).

[41] Jentsch, P. C., Anand, M. & Bauch, C. T. Prioritising COVID-19 vaccination in changing social and epidemiological landscapes: A mathematical modelling study. *The Lancet Infectious Diseases* **21**, 1097–1106 (2021).

[42] Rippinger, C. *et al.* Evaluation of undetected cases during the COVID-19 epidemic in Austria. *BMC Infectious Diseases* **21**, 70 (2021).

[43] Arashiro, T. *et al.* Coronavirus disease 19 (COVID-19) vaccine effectiveness against symptomatic severe acute respiratory syndrome coronavirus 2 (SARS-CoV-2) infection during Delta-dominant and Omicron-dominant periods in Japan: A multicenter prospective case-control study (Factors associated with SARS-CoV-2 infection and the effectiveness of COVID-19 vaccines study). *Clinical Infectious Diseases* **76** (2022).

[44] Kołodziej, B. & Pecka, I. Trudna sytuacja w szpitalach. Wstrzymane przyjęcia, coraz mniej wolnych łóżek [difficult situation in hospitals. Suspended admissions, fewer and fewer free beds] (2021). URL https://www.medonet.pl/koronawirus/koronawirus-w-polsce,koronawirus--brakuje-lozek-i-lekarzy--czwarta-fala-uderzyla-w-szpitale,artykul,58144898.html.

[45] Grove, C., Marinucci, A. & Montagni, I. Australian youth resilience and help-seeking during COVID-19: A cross-sectional study. *Behavioral Sciences* **13**, 121 (2023).

[46] Rewerska-Juśko, M. & Rejdak, K. Social stigma of patients suffering from COVID-19: Challenges for health care system. *Healthcare* **10**, 292 (2022).

[47] Tran, B. X. *et al.* Understanding health seeking behaviors to inform COVID-19 surveillance and detection in resource-scarce settings. *Journal of Global Health* **10**, 0203106 (2020).

[48] Wong, L. P. *et al.* The role of institutional trust in preventive practices and treatment-seeking intention during the coronavirus disease 2019 outbreak among residents in Hubei, China. *International Health* **14**, 161–169 (2022).

[49] Zheng, W., Kämpfen, F. & Huang, Z. Health-seeking and diagnosis delay and its associated factors: A case study on COVID-19 infections in Shaanxi Province, China. *Scientific Reports* **11**, 17331 (2021).

[50] Greene, S. K. *et al.* Nowcasting for real-time COVID-19 tracking in New York City: An evaluation using reportable disease data from early in the pandemic. *JMIR Public Health and Surveillance* **7** (2021).

[51] Spreco, A. *et al.* Nowcasting (short-term forecasting) of COVID-19 hospitalizations using syndromic healthcare data, Sweden, 2020. *Emerging Infectious Diseases* **28** (2022).

[52] Wu, J. T. *et al.* Nowcasting epidemics of novel pathogens: Lessons from COVID-19. *Nature Medicine* **27**, 388–395 (2021).

[53] Walkowiak, M. P. & Walkowiak, D. Underestimation in reporting excess COVID-19 death data in Poland during the first three pandemic waves. *International Journal of Environmental Research and Public Health* **19**, 3692 (2022).

[54] Sherratt, K. *et al.* Predictive performance of multi-model ensemble forecasts of COVID-19 across European nations. *eLife* **12** (2023).

[55] Grimm, V. *et al.* The ODD protocol for describing agent-based and other simulation models: A second update to improve clarity, replication, and structural realism. *Journal of Artificial Societies and Social Simulation* **23**, 7 (2020).

[56] Statistics Poland. Statistical yearbook of the republic of Poland (2019). URL https://stat.gov.pl/download/gfx/portalinformacyjny/pl/defaultaktualnosci/5515/2/19/1/rocznik_statystyczny_rzeczypospolitej_polskiej_2019.pdf.

[57] Li, M. Y. & Muldowney, J. S. Global stability for the SEIR model in epidemiology. *Mathematical Biosciences* **125**, 155–164 (1995).

[58] Sayampanathan, A. A. *et al.* Infectivity of asymptomatic versus symptomatic COVID-19. *The Lancet* **397**, 93–94 (2021).

[59] Han, D., Li, R., Han, Y., Zhang, R. & Li, J. COVID-19: Insight into the asymptomatic SARS-COV-2 infection and transmission. *International Journal of Biological Sciences* **16**, 2803–2811 (2020).

[60] Zhao, H., Lu, X., Deng, Y., Tang, Y. & Lu, J. COVID-19: asymptomatic carrier transmission is an underestimated problem. *Epidemiology and Infection* **148** (2020).

[61] Gold, J. A. W. *et al.* Characteristics and clinical outcomes of adult patients hospitalized with COVID-19 — Georgia, March 2020. *MMWR. Morbidity and Mortality Weekly Report* **69**, 545–550 (2020).

[62] Carrillo-Vega, M. F., Salinas-Escudero, G., García-Peña, C., Gutiérrez-Robledo, L. M. & Parra-Rodríguez, L. Early estimation of the risk factors for hospitalization and mortality by COVID-19 in Mexico. *PLOS ONE* **15** (2020).

[63] Petrilli, C. M. *et al.* Factors associated with hospital admission and critical illness among 5279 people with coronavirus disease 2019 in New York City: Prospective cohort study. *BMJ* (2020).

[64] Ko, J. Y. *et al.* Risk factors for coronavirus disease 2019 (COVID-19)–associated hospitalization: COVID-19–associated hospitalization surveillance network and behavioral risk factor surveillance system. *Clinical Infectious Diseases* **72** (2021).

[65] Twohig, K. A. *et al.* Hospital admission and emergency care attendance risk for SARS-CoV-2 delta (B.1.617.2) compared with alpha (B.1.1.7) variants of concern: A cohort study. *The Lancet Infectious Diseases* **22**, 35–42 (2022).

[66] National Institute of Public Health. Ogólnopolskie badanie seroepidemiologiczne COVID-19: OBSER-CO. Raport końcowy z badania [nationwide seroepidemiological study COVID-19: OBSER-CO. Final report.] (2023). Report at https://www.pzh.gov.pl/wp-content/uploads/2023/02/OBSERCO-Raport-koncowy-z-badania.pdf.

[67] Scobie, H. M. *et al.* Monitoring incidence of COVID-19 cases, hospitalizations, and deaths, by vaccination status—13 U.S. jurisdictions, April 4–July 17, 2021. *MMWR. Morbidity and Mortality Weekly Report* **70**, 1284–1290 (2021).

[68] Shahriari, B., Swersky, K., Wang, Z., Adams, R. P. & de Freitas, N. Taking the human out of the loop: A review of bayesian optimization. *Proceedings of the IEEE* **104**, 148–175 (2016).

[69] Lee, S. Y., Lei, B. & Mallick, B. Estimation of COVID-19 spread curves integrating global data and borrowing information. *PLOS ONE* **15** (2020).

[70] Postnikov, E. B. Estimation of COVID-19 dynamics "on a back-of-envelope": Does the simplest SIR model provide quantitative parameters and predictions? *Chaos, Solitons & Fractals* **135**, 109841 (2020).

[71] Bonifazi, G. *et al.* A study on the possible merits of using symptomatic cases to trace the development of the COVID-19 pandemic. *The European Physical Journal Plus* **136**, 481 (2021).

Supplementary Files

This is a list of supplementary files associated with this preprint. Click to download.

- Supplementary.pdf